

Heating Up Quadruply Quantized Vortices: Splitting Patterns and Dynamical Transitions

Shanquan Lan^{1,2,*}, Xin Li^{3,4,†}, Yu Tian^{5,6,‡}, Peng Yang^{5,§} and Hongbao Zhang^{7,||}

¹Department of Physics, Lingnan Normal University, Zhanjiang 524048, China

²Department of Physics, Peking University, Beijing 100871, China


³Department of Physics, University of Helsinki, P.O. Box 64, FI-00014 Helsinki, Finland

⁴Helsinki Institute of Physics, University of Helsinki, P.O. Box 64, FI-00014 Helsinki, Finland

⁵School of Physical Sciences, University of Chinese Academy of Sciences, Beijing 100049, China

⁶Institute of Theoretical Physics, Chinese Academy of Sciences, Beijing 100190, China

⁷Department of Physics, Beijing Normal University, Beijing 100875, China

 (Received 12 June 2023; revised 17 September 2023; accepted 2 November 2023; published 29 November 2023)

Using holographic duality, we investigate the impact of finite temperature on the instability and splitting patterns of quadruply quantized vortices, providing the first-ever analysis in this context. Through linear stability analysis, we reveal the occurrence of two consecutive dynamical transitions. At a specific low temperature, the dominant unstable mode transitions from the twofold rotational symmetry mode to the threefold one, followed by a transition from the threefold one to the fourfold one at a higher temperature. As the temperature is increased, we also observe the fivefold and sixfold rotational symmetry unstable modes get excited successively. Employing the full nonlinear numerical simulations, we further demonstrate that these two novel dynamical transitions, along with the temperature-induced instabilities for the fivefold and sixfold rotational symmetry modes, can be identified by examining the resulting distinct splitting patterns, which offers a promising route for the experimental verification in the cold atom gases.

DOI: [10.1103/PhysRevLett.131.221602](https://doi.org/10.1103/PhysRevLett.131.221602)

Introduction.—Superfluidity provides a unique manifestation of quantum mechanics at the macroscopic level, where the quantum many-body system can be described coherently by a complex valued order parameter. Quantized vortices, one of the hallmarks of superfluidity, are topological defects of the order parameter with a quantum number n multiple of 2π phase winding around the vortex center in superfluids, playing an important role in investigating the dynamics and properties of superfluids. It is the very presence of such topological defects that makes the quantum turbulence in superfluids exit the hydrodynamic description, in contrast to the classical turbulence in normal fluids. When the quantized vortices are far away from one another compared to the characteristic vortex size, they could be regarded approximately as point particles modeled by the Hall-Vinen-Iordanskii equation [1–3]. However, note that such quantized vortices are the gapped excited states with the corresponding energy proportional to the square of the winding number, so compared to the singly quantized vortex with $n = 1$, the multiply quantized vortices with $n \geq 2$ are generically unstable and will split into many singly quantized vortices. Not only does the splitting dynamics provide an avenue to generate quantum turbulence on the large scale, but it also offers us an opportunity as well as a challenge to study the vortex dynamics in an extreme regime where the whole physical process occurs on the scale of the size of a vortex core. Since the creation of multiply quantized vortices achieved

in gaseous cold atoms by topological phase imprinting [4–6], Laguerre-Gaussian beams [7], and laser beam spiraling around an obstacle [8], the instability and the splitting patterns of multiply quantized vortices have been extensively studied [9–26], where it is found that the vortex of the winding number $n \geq 2$ generically exhibits the splitting instability of p -fold rotational symmetry with $p = 2, \dots, 2(n - 1)$.

Of particular interest are quadruply quantized ($n = 4$) vortices [19–26]. On the one hand, different from doubly quantized ones, quadruply quantized vortices, as alluded above, have more than one ($p = 2, 3, 4, 5, 6$) splitting channels, which compete with one another and lead to much richer scenarios. On the other hand, compared to other multiply quantized vortices with $n > 2$, the quadruply quantized vortices can be readily manipulated in gaseous cold atoms. For zero temperature Bose gases, it is shown for the quadruply quantized vortices by the Gross-Pitaevskii equation (GPE) that the corresponding growing rates for each splitting channel vary with the scattering length [19,20]. But due to the narrow region of the scattering length as well as the tiny value of the growing rate for $p = 4, 5, 6$ splitting channel, only $p = 2, 3$ splitting patterns have been observed experimentally [20–22].

However, there are two obvious deficiencies associated with the previous theoretical modeling. One is the strong coupling limit, which corresponds to the infinite scattering length and cannot be well addressed by GPE. The other is

the finite temperature effect, which comes from the ambient surrounding as a thermal bath and can only be incorporated into GPE by adding some dissipative terms phenomenologically. These two shortcomings can be well overcome by holographic duality, which is an alternative theoretical framework to encode the strongly coupled finite temperature quantum many-body systems into the gravitational systems of black holes with one extra dimension [27–29]. In particular, since its advent [30,31], the holographic model of superfluids has been applied to a variety of scenarios related to superfluid dynamics, including the dynamics associated with the topological defects [32–44], and quantum turbulence [45–48].

In this Letter, we intend to investigate the impact of finite temperature on the splitting process of a quadruply quantized vortex by the holographic superfluid model. Among others, not only do we find that the growing rate gets enhanced to a maximum for each unstable mode by heating the superfluid up to some intermediate temperatures below the critical one, but we also discover there exist two distinct temperatures for novel dynamical transitions, where the splitting pattern transits from twofold rotational symmetry to threefold and from threefold rotational symmetry to fourfold, respectively.

Holographic superfluid model.—The action of the two dimensional holographic superfluid model is given by [30,31]

$$S = \int_M \sqrt{-g} d^4x \left[\frac{1}{16\pi G} \left(R + \frac{6}{L^2} \right) - \frac{1}{q^2} \left(\frac{1}{4} F^2 + |D\Psi|^2 + m^2 |\Psi|^2 \right) \right], \quad (1)$$

where G is the Newton's gravitational constant, R is the Ricci scalar, L is the anti-de Sitter (AdS) radius, $D_\mu \Psi = (\nabla_\mu - iA_\mu)\Psi$, A_μ is a U(1) gauge field, and Ψ is a complex scalar field with mass m and charge q .

We shall work with the probe approximation, which is achieved by taking a large q limit. Accordingly, the backreaction of the matter fields onto the background geometry is negligible. For our purpose, the background geometry is fixed as the Schwarzschild-AdS black hole

$$ds^2 = \frac{L^2}{z^2} \left(-f(z) dt^2 + \frac{1}{f(z)} dz^2 + dx^2 + dy^2 \right), \quad (2)$$

where $f(z) = 1 - (z/z_h)^3$ with z_h the black hole horizon and $z = 0$ the AdS boundary. The Hawking temperature of the black hole is

$$T = \frac{3}{4\pi z_h}, \quad (3)$$

which is also identified as the temperature of the dual boundary system. The equations of motion for the matter

fields are given by

$$D^\mu D_\mu \Psi - m^2 \Psi = 0, \quad \nabla_\mu F^{\mu\nu} = J^\nu, \quad (4)$$

with $J^\nu = i(\Psi^* D^\nu \Psi - \Psi D^{\nu*} \Psi^*)$.

Without loss of generality, we set $L = 1$, $z_h = 1$, and $m^2 = -2$. By adopting the axial gauge $A_z = 0$, the asymptotic behaviors of the matter fields near the boundary are

$$\Psi \equiv z\Phi = z(\psi_- + \psi_+ z + \dots), \\ A_\mu = a_\mu + b_\mu z + \dots \quad (5)$$

According to the holographic dictionary, ψ_- corresponds to the source and ψ_+ is the condensate response to the source. In addition, $a_t = \mu$ corresponds to the chemical potential with $-b_t = \rho$ the particle number density.

For an isotropic uniform static superfluid system, there exists a critical chemical potential $\mu_c = \rho_c = 4.064$, above which the scalar field with the source ψ_- turned off can have a nontrivial solution besides the trivial one $\Psi = 0$, signaling a phase transition from the normal fluid phase to the superfluid phase. In order to investigate the temperature effect on the superfluid dynamics, we fix the total particle number of our boundary system instead of fixing $z_h = 1$, which can be achieved simply by resorting to the scaling symmetry of the bulk dynamics

$$z_h \rightarrow \sigma z_h, \quad T \rightarrow \frac{T}{\sigma}, \quad (t, x, y, z) \rightarrow \sigma(t, x, y, z), \\ \mu \rightarrow \frac{\mu}{\sigma}, \quad \rho \rightarrow \frac{\rho}{\sigma^2}, \quad \psi_+ \rightarrow \frac{\psi_+}{\sigma^2}. \quad (6)$$

Accordingly, the above phase transition can be rephrased as occurring at a certain critical temperature T_c .

The quadruply quantized vortex and its linear instability.—To obtain the static vortex configuration, which is axisymmetric, we would like to work with the polar coordinates. The background metric is rewritten as

$$ds^2 = \frac{1}{z^2} \left[-f(z) dt^2 + \frac{1}{f(z)} dz^2 + dr^2 + r^2 d\theta^2 \right]. \quad (7)$$

The corresponding ansatz for the nonvanishing matter fields is given by

$$\Phi = \psi(z, r) e^{in\theta}, \quad A_t = A_t(z, r), \quad A_\theta = A_\theta(z, r), \quad (8)$$

where n is the winding number of the quantized vortex. Substituting the above expressions into Eq. (4), we obtain the equations of motion for a quantized vortex, which can be solved numerically by the pseudospectral method. Please refer to Supplemental Material [49] for numerical details. As a demonstration, we plot the configuration of our quadruply quantized vortex at temperature $T/T_c = 0.636$ in the upper panel of Fig. 1.

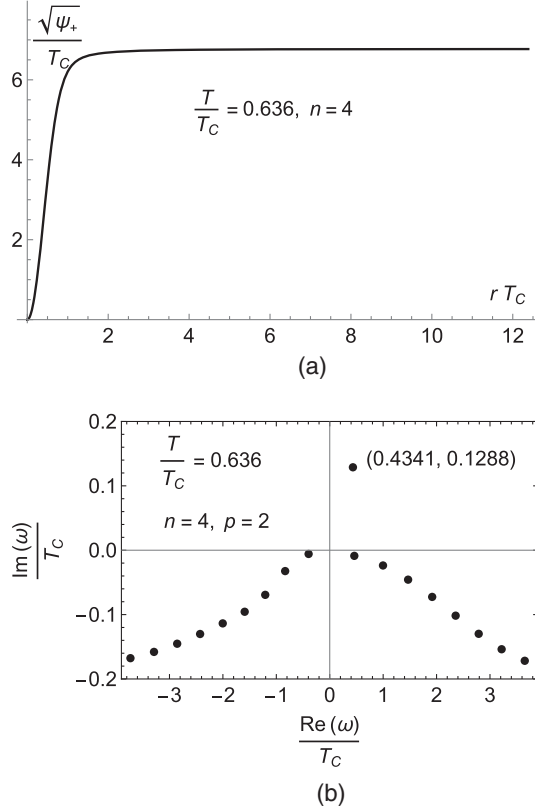


FIG. 1. (a) The configuration of a quadruply quantized vortex at temperature $T/T_c = 0.636$. (b) The low lying spectrum of quasinormal modes (ω) for $p = 2$ of the vortex in the upper panel.

Now we are going to investigate the linear instability of the resulting quadruply quantized vortex by calculating its quasinormal modes. To proceed, we prefer to go from the Schwarzschild coordinates to the Eddington-Finkelstein coordinates, in which the background metric takes the following form:

$$ds^2 = \frac{1}{z^2} [-f(z)dt^2 - 2tdtdz + dr^2 + r^2d\theta^2]. \quad (9)$$

After this coordinate transformation, $A_z = [A_t(z, r)/f(z)]$. In order to preserve the axial gauge $A_z = 0$ in the above new coordinates, we are required to perform the following gauge transformation:

$$\psi(z, r) \rightarrow e^{i\lambda(z, r)}\psi(z, r), \quad A_r(z, r) = \partial_r\lambda(z, r), \quad (10)$$

with $\lambda(z, r) = -\int_0^z [A_t(z, r)/f(z)]dz$.

Since the resulting vortex configuration possesses the time translation symmetry and rotation symmetry, the linear perturbations of the matter fields can be constructed as

$$\begin{aligned} \delta\Phi &= e^{in\theta} [\delta\psi_1(z, r)e^{-i\omega t + ip\theta} + \delta\psi_2^*(z, r)e^{i\omega^* t - ip\theta}], \\ \delta A_\mu &= \delta A_\mu(z, r)e^{-i\omega t + ip\theta} + \delta A_\mu^*(z, r)e^{i\omega^* t - ip\theta}. \end{aligned} \quad (11)$$

Substituting the above expressions into Eq. (4), we obtain the linear perturbation equations, which together with a set of boundary conditions at the AdS boundary as well as the regular boundary conditions at the black hole horizon can be cast into the matrix form $\mathcal{A}(\omega, p)\delta = \mathcal{B}(\omega, p)$ for the linear perturbations abbreviated as δ . The frequency of the quasinormal modes for each azimuthal number p can be obtained numerically by solving the generalized eigenvalue problem. Generically, the quasinormal frequencies are complex. In particular, if there exists a quasinormal frequency with a positive imaginary part, then the system is unstable. The larger the positive imaginary part is, the more unstable the system is. We demonstrate the low lying spectrum of quasinormal modes for $p = 2$ in our quadruply quantized vortex at $T/T_c = 0.636$ in the bottom panel of Fig. 1. As one can see, the dominant mode is given by a quasinormal frequency with a positive imaginary part, indicating the instability of the corresponding quadruply quantized vortex for $p = 2$ channel.

We plot the temperature dependence of the imaginary part of the dominant mode in Fig. 2 for $p = 2, 3, 4, 5, 6$ channels. First, the dominant mode for each channel displays a universal bell curve behavior, namely the imaginary part rises with the increase of temperature, peaks at a certain temperature, and then drops universally to zero as the temperature is cranked up to the critical one. This may be understood intuitively in the following way. Actually associated with the temperature, there are two factors in action. One is the thermal dissipation, and the other is the vortex size. As the temperature is increased, not only is the thermal dissipation enhanced [43], but also the vortex size characterized by the healing length is enlarged. The enhanced thermal dissipation tends to make the vortex unstable while the enlarged vortex size serves as an obstacle against the thermal induced instability. As a result, the thermal dissipation wins at low temperatures but taken over by the vortex size at high temperatures. In particular, near the critical temperature, the vortex size gets divergent, leading to the vanishing imaginary part over there, consistent with the numerical result presented in Fig. 2.

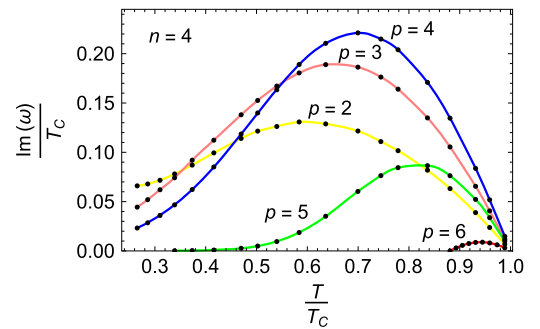


FIG. 2. The variation of the imaginary part of the dominant mode of the quadruply quantized vortex with the temperature for $p = 2, 3, 4, 5, 6$.

Second, although $p = 2, 3, 4$ channel instability occurs in the full temperature regime available by our numerics from $T/T_c = 0.265$ to $T/T_c = 0.989$, there exist threshold temperatures $T/T_c = 0.34$ and $T/T_c = 0.88$ for $p = 5, 6$ channel instability, respectively. But nevertheless, this finding promises a precious new window to observe $p = 5, 6$ channel splitting at high temperatures. Third, at $T/T_c \lesssim 0.35$, the most unstable mode corresponds to the $p = 2$ dominant mode, while at $T/T_c \gtrsim 0.55$, the most unstable mode is given by the $p = 4$ dominant mode. The $p = 3$ dominant mode serves as the most unstable mode in between. This result signals two dynamic transitions from $p = 2$ to $p = 3$ channel splitting at $T/T_c = 0.35$ and from $p = 3$ to $p = 4$ channel splitting at $T/T_c = 0.55$, respectively for the splitting of our quadruply quantized vortex. In what follows, we shall substantiate the above two important implications by visualizing the real time splitting process of our quadruply quantized vortex.

Full nonlinear numerical simulations and splitting patterns of quadruply quantized vortex.—The real time splitting process of our quadruply quantized vortex can be implemented by full nonlinear numerical simulations of the $3 + 1$ dimensional bulk dynamics. To improve the numerical accuracy for such simulations, we shall work with the rectangular coordinates rather than the polar coordinates. The rectangular Eddington-Finkelstein metric reads

$$ds^2 = \frac{1}{z^2} [-f(z)dt^2 - 2tdtdz + dx^2 + dy^2], \quad (12)$$

where the equations of motion for the bulk matter fields can be written explicitly as the constraint equation

$$\partial_z(\partial_z A_t - \partial \cdot \mathbf{A}) = i(\bar{\Phi}\partial_z \Phi - \Phi\partial_z \bar{\Phi}), \quad (13)$$

and the evolution equations

$$\begin{aligned} \partial_t \partial_z A_t &= \partial^2 A_t + f \partial_z \partial \cdot \mathbf{A} - \partial_t \partial \cdot \mathbf{A} - 2A_t \bar{\Phi} \Phi \\ &\quad + if(\bar{\Phi}\partial_z \Phi - \Phi\partial_z \bar{\Phi}) - i(\bar{\Phi}\partial_t \Phi - \Phi\partial_t \bar{\Phi}), \\ \partial_t \partial_z \Phi &= iA_t \partial_z \Phi + \frac{1}{2}[i\partial_z A_t \Phi + f\partial_z^2 \Phi \\ &\quad + f'\partial_z \Phi + (\partial - iA)^2 \Phi - z\Phi], \\ \partial_t \partial_z \mathbf{A} &= \frac{1}{2}[\partial_z(\partial A_t + f\partial_z \mathbf{A}) + (\partial^2 \mathbf{A} - \partial \partial \cdot \mathbf{A}) \\ &\quad - i(\bar{\Phi}\partial \Phi - \Phi\partial \bar{\Phi})] - \mathbf{A}\bar{\Phi}\Phi. \end{aligned} \quad (14)$$

With the boundary conditions documented in Supplemental Material [49], the long time stable numerical simulation can be achieved by solving A_t through the constraint equation and evolving Φ and \mathbf{A} via the fourth order Runge-Kutta method.

We first present the splitting processes of the quadruply quantized vortex at different temperatures in Fig. 3, where the initial value is specified as the quadruply quantized

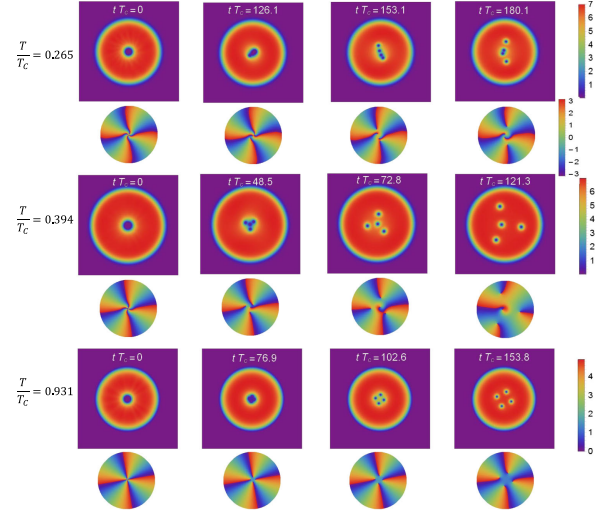


FIG. 3. Density and phase plots of the condensate for splitting processes of the quadruply quantized vortex under random perturbations with distinct splitting patterns at different temperatures.

vortex perturbed by random noise, i.e.,

$$\Phi = e^{in\theta} \psi(z, r) \left(1 + \sum_{p=1}^N [\alpha(p)e^{-ip\theta} + \beta(p)e^{ip\theta}] \right), \quad (15)$$

where $\alpha(p)$ and $\beta(p)$ are randomly chosen small constants between $(-0.002, 0.002)$, and N is a truncation integer we choose as 20. Depending on the temperature, the splitting processes display different splitting patterns of p -fold rotational symmetry, which is completely consistent with the previous linear instability analysis. At the low temperature $T/T_c = 0.265$, the $p = 2$ splitting pattern dominates. At the intermediate temperature $T/T_c = 0.394$, the $p = 3$ splitting pattern dominates. At the high temperature $T/T_c = 0.931$, the $p = 4$ splitting pattern dominates. To the best of our knowledge, only $p = 2, 3$ splitting patterns have been revealed at near-zero temperature condition so far [20–22]. Our discovery indicates that $p = 4$ splitting pattern promises to be observed in cold atom gases by tuning up the temperature.

Taking into account that neither $p = 5$ nor $p = 6$ channel linear instability is dominant, so in order to see $p = 5, 6$ splitting pattern at the full nonlinear level, we had better give up on the previous random perturbation. Instead, we prepare the initial quadruply quantized vortex perturbed under $p = 5$ and $p = 6$ type perturbation separately, i.e.,

$$\Phi = e^{in\theta} \psi(z, r) (1 + \alpha e^{ip\theta} + \beta e^{-ip\theta}), \quad (16)$$

with α and β small constants. The resulting splitting processes are presented in Fig. 4. As one can see, the $p = 5$ splitting pattern displays five $n = 1$ quantized vortices rotating around one $n = -1$ antivortex. On the other hand, the $p = 6$ splitting pattern dominates in the early stage with six vortices surrounding two antivortices.

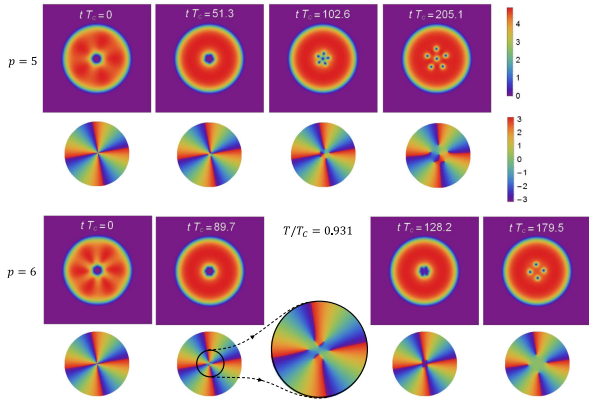


FIG. 4. Density and phase plots of the condensate for splitting processes of the quadruply quantized vortex under $p = 5, 6$ type perturbations at temperature $T/T_c = 0.931$, where six vortices are clearly seen to surround two antivortices from the close-up of the phase plot.

But after the annihilation of the two vortex pairs, the system ends up with the $p = 4$ splitting pattern. This is consistent with the previous linear stability analysis, where the imaginary part of $p = 6$ dominant mode, as displayed in Fig. 2, is much smaller than that of $p = 4$ dominant mode. By tuning up the temperature and specifying the perturbation, our simulation provides the first numerical evidence for $p = 5, 6$ splitting patterns of the quadruply quantized vortex, which have never been accomplished before in any other numerical simulation. In particular, our finding indicates that it is also feasible to observe $p = 5$ (even $p = 6$) splitting pattern of the quadruply quantized vortex in cold atom gases if the experimental setup is cautiously conducted.

Conclusion.—Compared to the conventional theoretical models, which have significant limitations and shortcomings in addressing the finite temperature effect, holographic duality provides us with a well-defined description of the finite temperature superfluid by geometrizing it as a bulk hairy black hole. Through the lens of holography, we have investigated the temperature effect on the instability and splitting patterns of the quadruply quantized vortex by both linear perturbation analysis and full nonlinear simulations. As a result, the growing rate for each mode turns out to be enhanced to a maximal value at a certain temperature below the critical one. In particular, such an enhancement is appreciable for $p = 4$ and $p = 5$ modes, making the associated splitting patterns also clearly visible in our numerical simulations. In addition, by heating up our superfluid, we also reveal two successive dynamical transitions, one from $p = 2$ splitting pattern to $p = 3$ splitting pattern, followed by the other from $p = 3$ to $p = 4$.

Note that the finite temperature dynamics of the quantized vortices in superfluids has recently become amenable

to being manipulated in a controllable manner due to the great experimental advances in cold atom gases [50,51]. In light of this, our sharp predictions show great promise to be tested in the real tabletop experiments. In addition, as demonstrated in Supplemental Material [49], while we focus on quadruply quantized vortices due to their experimental relevance, our model predicts similar behaviors more generally for multiply quantized vortices with $n > 2$. In particular, increasing the temperature favors decay channels with higher p -fold rotational symmetry. We conclude by pointing out that the probe approximation is reliable in the regime $T/T_c > 0.25$ we work with. But one is required to take into account the back-reaction of the matter fields onto the metric when approaching lower temperatures.

This work is partly supported by the National Key Research and Development Program of China Grant No. 2021YFC2203001, National Natural Science Foundation of China (Grants No. 12005088, No. 11975235, No. 12035016, and No. 12075026), and Guangdong Basic and Applied Basic Research Foundation of China (Grant No. 2022A1515011938). S.L. acknowledges the support from Lingnan Normal University Project (Grants No. YL20200203 and No. ZL1930). X.L. acknowledges the support from China Scholarship Council (CSC No. 202008610238).

*lansq@lingnan.edu.cn

†xin.z.li@helsinki.fi

‡ytian@ucas.ac.cn

§yangpeng18@mails.ucas.ac.cn

||hongbaozhang@bnu.edu.cn

- [1] H. E. Hall and W. F. Vinen, *Proc. R. Soc. A* **238**, 204 (1956).
- [2] S. V. Iordanskii, *Ann. Phys. (N.Y.)* **29**, 335 (1964).
- [3] S. V. Iordanskii, *J. Exp. Theor. Phys.* **22**, 160 (1966), <http://www.jetp.ras.ru/cgi-bin/e/index/rt/49/1/p225?a=list>.
- [4] T. Isoshima, M. Nakahara, T. Ohmi, and K. Machida, *Phys. Rev. A* **61**, 063610 (2000).
- [5] A. E. Leanhardt, A. Görlitz, A. P. Chikkatur, D. Kielpinski, Y. Shin, D. E. Pritchard, and W. Ketterle, *Phys. Rev. Lett.* **89**, 190403 (2002).
- [6] M. Möttönen, V. Pietilä, and S. M. M. Virtanen, *Phys. Rev. Lett.* **99**, 250406 (2007).
- [7] M. F. Andersen, C. Ryu, P. Cladé, V. Natarajan, A. Vaziri, K. Helmerson, and W. D. Phillips, *Phys. Rev. Lett.* **97**, 170406 (2006).
- [8] K. E. Wilson, E. C. Samson, Z. L. Newman, and B. P. Anderson, *Phys. Rev. A* **106**, 033319 (2022).
- [9] Y. Shin, M. Saba, M. Vengalattore, T. A. Pasquini, C. Sanner, A. E. Leanhardt, M. Prentiss, D. E. Pritchard, and W. Ketterle, *Phys. Rev. Lett.* **93**, 160406 (2004).
- [10] J. A. M. Huhtamäki, M. Möttönen, T. Isoshima, V. Pietilä, and S. M. M. Virtanen, *Phys. Rev. Lett.* **97**, 110406 (2006).
- [11] A. Muñoz Mateo and V. Delgado, *Phys. Rev. Lett.* **97**, 180409 (2006).

- [12] K. J. H. Law, L. Qiao, P. G. Kevrekidis, and I. G. Kevrekidis, *Phys. Rev. A* **77**, 053612 (2008).
- [13] K. Gawryluk, T. Karpiuk, M. Brewczyk, and K. Rzazewski, *Phys. Rev. A* **78**, 025603 (2008).
- [14] H. M. Nilsen and E. Lundh, *Phys. Rev. A* **77**, 013604 (2008).
- [15] M. Takahashi, V. Pietilä, M. Möttönen, T. Mizushima, and K. Machida, *Phys. Rev. A* **79**, 023618 (2009).
- [16] S. Ishino, M. Tsubota, and H. Takeuchi, *Phys. Rev. A* **88**, 063617 (2013).
- [17] A. Prem, S. Moroz, V. Gurarie, and L. Radzihovsky, *Phys. Rev. Lett.* **119**, 067003 (2017).
- [18] P. Kuopanportti, S. Bandyopadhyay, A. Roy, and D. Angom, *Phys. Rev. A* **100**, 033615 (2019).
- [19] Y. Kawaguchi and T. Ohmi, *Phys. Rev. A* **70**, 043610 (2004).
- [20] T. Isoshima, M. Okano, H. Yasuda, K. Kasa, J. A. M. Huhtamäki, M. Kumakura, and Y. Takahashi, *Phys. Rev. Lett.* **99**, 200403 (2007).
- [21] T. Kuwamoto, H. Usuda, S. Tojo, and T. Hirano, *J. Phys. Soc. Jpn.* **79**, 034004 (2010).
- [22] H. Shibayama, A. Tsukada, T. Yoshihara, and T. Kuwamoto, *J. Phys. Soc. Jpn.* **85**, 054401 (2016).
- [23] P. Kuopanportti and M. Möttönen, *Phys. Rev. A* **81**, 033627 (2010).
- [24] J. Rabinä, P. Kuopanportti, M. I. Kivioja, M. Möttönen, and T. Rossi, *Phys. Rev. A* **98**, 023624 (2018).
- [25] Q. Zhu and L. Pan, *J. Low Temp. Phys.* **203**, 392 (2021).
- [26] G. D. Telles, P. E. S. Tavares, A. R. Fritsch, A. Cidrim, and V. S. Bagnato, *Laser Phys. Lett.* **19**, 015501 (2022).
- [27] J. M. Maldacena, *Int. J. Theor. Phys.* **38**, 1113 (1999).
- [28] S. S. Gubser, I. R. Klebanov, and A. M. Polyakov, *Phys. Lett. B* **428**, 105 (1998).
- [29] E. Witten, *Adv. Theor. Math. Phys.* **2**, 253 (1998).
- [30] S. A. Hartnoll, C. P. Herzog, and G. T. Horowitz, *Phys. Rev. Lett.* **101**, 031601 (2008).
- [31] S. A. Hartnoll, C. P. Herzog, and G. T. Horowitz, *J. High Energy Phys.* **12** (2008) 015.
- [32] V. Keränen, E. Keski-Vakkuri, S. Nowling, and K. P. Yogendran, *Phys. Rev. D* **81**, 126011 (2010).
- [33] V. Keränen, E. Keski-Vakkuri, S. Nowling, and K. P. Yogendran, *Phys. Rev. D* **81**, 126012 (2010).
- [34] V. Keränen, E. Keski-Vakkuri, S. Nowling, and K. P. Yogendran, *New J. Phys.* **13**, 065003 (2011).
- [35] A. Salvio, *J. High Energy Phys.* **09** (2012) 134.
- [36] S. Lan, W. Liu, and Y. Tian, *Phys. Rev. D* **95**, 066013 (2017).
- [37] C. Xia, H. Zeng, H. Zhang, Z. Nie, Y. Tian, and X. Li, *Phys. Rev. D* **100**, 061901(R) (2019).
- [38] S. Lan, G. Li, J. Mo, and X. Xu, *J. High Energy Phys.* **02** (2019) 122.
- [39] X. Li, Y. Tian, and H. Zhang, *J. High Energy Phys.* **02** (2020) 104.
- [40] M. Guo, E. Keski-Vakkuri, H. Liu, Y. Tian, and H. Zhang, *Phys. Rev. Lett.* **124**, 031601 (2020).
- [41] P. Wittmer, C. Schmied, T. Gasenzer, and C. Ewerz, *Phys. Rev. Lett.* **127**, 101601 (2021).
- [42] C. Ewerz, A. Samberg, and P. Wittmer, *J. High Energy Phys.* **11** (2021) 199.
- [43] Y. Yan, S. Lan, Y. Tian, P. Yang, S. Yao, and H. Zhang, *Phys. Rev. D* **107**, L121901 (2023).
- [44] S. Lan, X. Li, J. Mo, Y. Tian, Y. Yan, P. Yang, and H. Zhang, *J. High Energy Phys.* **05** (2023) 223.
- [45] A. Adams, P. M. Chesler, and H. Liu, *Science* **341**, 6144 (2013).
- [46] C. Ewerz, T. Gasenzer, M. Karl, and A. Samberg, *J. High Energy Phys.* **05** (2015) 070.
- [47] Y. Du, C. Niu, Y. Tian, and H. Zhang, *J. High Energy Phys.* **12** (2015) 018.
- [48] S. Lan, Y. Tian, and H. Zhang, *J. High Energy Phys.* **07** (2016) 092.
- [49] See Supplemental Material at <http://link.aps.org/supplemental/10.1103/PhysRevLett.131.221602> for more details on our numerics as well as the relevant numerical results for the instability and splitting of triply quantized vortices.
- [50] Y. P. Sachkou, C. G. Baker, G. I. Harris, O. R. Stockdale, S. Forstner, M. T. Reeves, X. He, D. L. Mcauslan, A. S. Bradley, M. J. Davis, and W. P. Bowen, *Science* **366**, 1480 (2019).
- [51] W. J. Kwon, G. Del Pace, K. Xhani, L. Galantucci, A. Muzi Falconi, M. Inguscio, F. Scazza, and G. Roati, *Nature (London)* **600**, 64 (2021).